Impact of GNSS radio occultation bending angle data assimilation in YH4DVAR system*

Zhu Meng-Bin(朱孟斌)†, Zhang Wei-Min(张卫民), Cao Xiao-Qun(曹小群), and Yu Yi(余 意)

College of Computer, National University of Defense Technology, Changsha 410073, *China*

(Received 9 September 2013; revised manuscript received 2 December 2013; published online 20 April 2014)

Global Navigation Satellite System (GNSS) radio occultation measurements have been assimilated into the four-dimensional variational data assimilation system (YH4DVAR) using a one-dimensional bending angle operator (GBAO) as a new type of observation. For the sake of verifying the impact of GNSS radio occultation (RO) measurements to the data assimilation system, three experiments have been conducted. The statistical results of the analysis error experiment and forecast skill experiment show that the GNSS RO measurements have an impact on the analysis system. The typhoon forecast experiment shows the impact on the important weather process. They all have a positive impact on the weather forecast. Lastly, we look forward to future work on the observation system simulation experiment (OSSE) to investigate the impact of GNSS RO measurements as a function of observation number, which is an effective method to estimate the saturation of the observation number.

Keywords: GNSS radio occultation, analysis field biases experiment, forecast skill experiment, typhoon forecast impact experiment

PACS: 92.60.hv, 92.60.Wc, 95.10.Gi, 04.20.Fy **DOI:** 10.1088/1674-1056/23/6/069202

1. Introduction

GNSS RO data assimilation technology has been developing since 1995.[1] With the hard work of scientific researchers, various algorithms are developed for different kinds of GNSS RO data, including local and non-local refractivity operators for GNSS RO refractivity observations,[2] and one-dimensional and two-dimensional bending angle operators.[3,4] Every algorithm has its own advantages and disadvantages. Generally, bending angle data have more advantages than refractivity data, and bending angle data assimilation is the preference direction of GNSS RO data assimilation. The research of GNSS RO data assimilation technology is accelerated by the launch of the Constellation Observing System for Meteorology, Ionosphere, and Climate (COSMIC) satellites in 2006[5] and the GNSS Receiver for Atmospheric Sounding (GRAS) instrument on Metop-A/B.

The data assimilation system WRFDA, which is accompanied with the world famous open source numerical weather prediction system WRF, gives a simple implementation of GNSS RO refractivity data assimilation operator on model levels. We completed a one-dimensional bending angle operator on the basis of the local refractivity operator in WRFDA. And bending angle observations can be assimilated in WRF three-dimensional variational data assimilation system on model levels. The one-dimensional bending angle operator was simultaneously implemented in YH4DVAR.[6–9] The bending angle data assimilation is performed on observation levels with geopotential height considered in four-dimensional variational data assimilation system rather than three-dimensional variational data assimilation system.

Europe and the United States have been researching GNSS RO data assimilation for a long time. Cucurull in National Centers for Environmental Prediction (NCEP) researched the variational data assimilation method to introduce bending angle observation data into Global Forecasting System (GFS).[10] In Cucurull's paper, a one-dimensional bending angle operator (NBAM) is given and the weather forecast skill of operational system is improved by the operator.

In 2006. the European Center for Medium-range Weather Forecasts (ECMWF) implemented a one-dimensional bending angle operator in their operational four-dimensional variational data assimilation system.[3] A sixty-days forecast impact experiment has been done and the results show that GNSS RO bending angle data can improve the accuracy of the temperature forecast and reduce the root-mean-square (RMS) error of the temperature forecast, especially in the Southern Hemisphere from the height of 300 hPa to 50 hPa. Soon afterwards, ECMWF began the research of two-dimensional bending angle operator and has done a series of experiments.[4]

The observation sensitivity experiment gives the contribution of various observation data to the ECMWF operational data assimilation system. It shows that the contribution of GNSS RO data is just less than that of AMSU-A and IASI, but more than that of AIREP and AIRS.[11] Figure 1 shows the impact of ECMWF observation control experiment. The improvement of temperature and geopotential height at 100 hPa

*Project supported by the National Natural Science Foundation of China (Grant Nos. 40775064, 41105063, and 41375113) and the Special Scientific Research Fund of Meteorological Public Welfare Profession of China (Grant Nos. GYHY201006015 and GYHY201206007).

†Corresponding author. E-mail: zhumengbin@nudt.edu.cn

© 2014 Chinese Physical Society and IOP Publishing Ltd

in the ECMWF observation control experiment is obvious because of the introduction of GNSS RO data.[12]

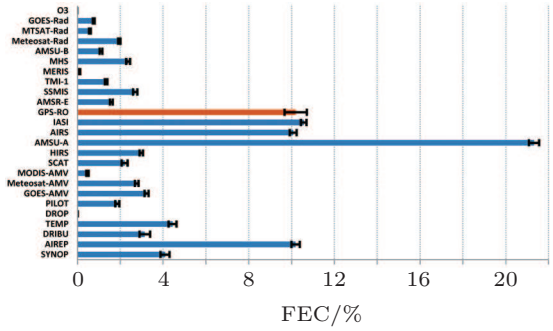

Fig. 1. (color online) ECMWF various observations contributions to the Numerical Weather Prediction (NWP) System.[11]

In this study, we conducted a series of experiments and analyses to evaluate the contribution and impact that GNSS RO observations could have on numerical weather forecasts in YH4DVAR system[7]. Section 2 gives the introduction of GNSS RO experiment data and the experiment environment. Two observation impact experiments are described in Section 3, and the GNSS RO impact on numerical weather prediction is shown. Section 4 describes a weather process impact experiment. Typhoon "BOLAVEN" was simulated. Section 5 summarizes the main conclusions and discusses the future plan of GNSS RO measurements research.

2. Experiment data and environment

2.1. Experiment data

The GNSS RO observations assimilated in the data assimilation experiments in this research are from various global RO constellation systems, including COSMIC, METOP-A/GRAS, GRACE-A, TerraSAR-X, and C/NOFS. They provide a number of about 2200 profiles per day in total, which are globally distributed. One of the COSMIC satellites has broken-down and could no longer offer observations. GRAS launched by EUMETSAT is the only complete operational constellation on orbit. The GRAS instrument on METOP-A offers 600 GNSS RO profiles per day, which started in October 2006. METOP-B was launched in the second half year of 2012. From early 2013, the GRAS instrument on METOP-B is now providing 700 global distributed profiles per day, but the profiles METOP-B offers are not used as experiment data in this research. GRACE-A, TerraSAR-X, and C/NOFS have all served for science experiments, and can also be used for operational NWP system.

There are about 650 GNSS RO observation profiles distributed globally in a 6-hour window, which is shown in Fig. 2. Every GNSS RO observation profile has 300 vertical levels. After being thinned for reduction of the vertical correlation, the profiles become 68 levels in the YH4DVAR system.

A 24-hour global GNSS RO profiles distribution is shown in Fig. 3. The density of the profiles in polar zones and tropical zone is low. We have done a statistical experiment to confirm that the GNSS RO profiles distribution varies with the latitude. The results of experiment are shown in Fig. 4. It has been demonstrated that the variation is related to the orbit parameters and occultation time.

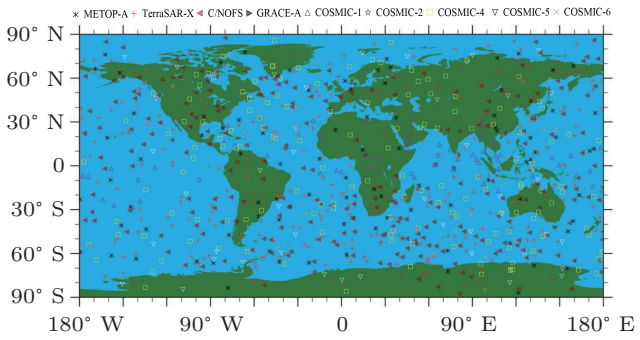

Fig. 2. (color online) GNSS RO measurements distribution in 6-hour window (Global).

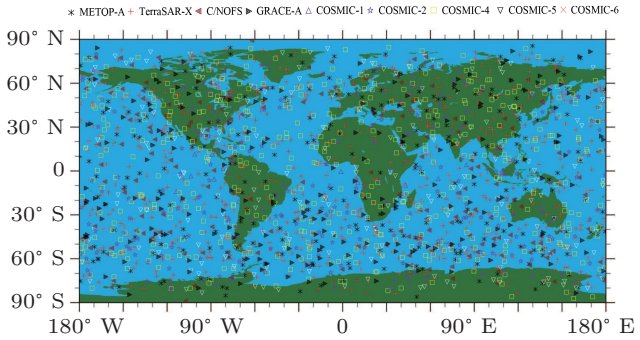

Fig. 3. (color online) GNSS RO measurements distribution in 24-hour window (Global).

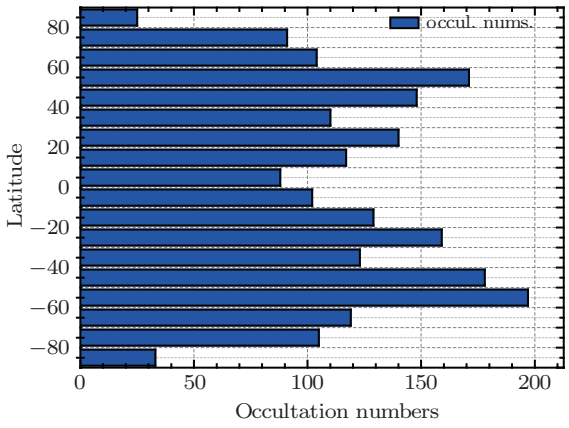

Fig. 4. (color online) GNSS RO measurements distribution varies with latitude (TIME: 20120815).

2.2. Experiment environment

The forward operator of one-dimensional (1D) bending angle in YH4DVAR uses the best average refractivity coefficients in Ref. [13] and considers the non-ideal gas condition in atmosphere to calculate refractivity, which would consequently be more accurate. We designed a latitude and altitude

related observation error model, which is referred to the bending angle observations error statistical experiment. The details are given by Ref. [9].

The bending angle is the radio path that is caused by the radio from GNSS satellite to Low Earth Orbit (LEO) satellite. Without considering the horizontal gradient in the through path of radio, the equation of 1D GNSS bending angle operator described in Ref. [9] is given as Eq. (1) with the assumption that the atmosphere distribution is spherical symmetric

$$\alpha = H_\alpha F_{\rm I} H_{\rm N}(T,p,q). \tag{1}$$

The $H_{\rm N}(T,p,q)$ term is used to calculate the refractivities with temperature, pressure, humidity, and geopotential height on the model grids. $F_{\rm I}$ interpolates the refractivity values on model grids to the tangent point of the ray trace. H_α calculates the bending angle values using Abel transform with the refractivity values on the tangent point of the ray trace. The Abel transform is demonstrated as follows:

$$\alpha(a) = -2a\int_{r_t}^{\infty} \frac{1}{\sqrt{r^2n^2 - a^2}} \frac{{\rm d}\ln(n)}{{\rm d}r}\,{\rm d}r. \tag{2}$$

This represents that the bending angle value has one-to-one correspondent relations with the refractivity index, which is the function of radius.

With the designed observation error model in Ref. [9], the analysis fields have been generated again for the period from 1 August 2012 to 31 August 2012. A statistical test has been done for the fractional differences of the standard deviations of bending angle between GNSS RO and model simulations. This is based on the fractional bending angle differences between GNSS RO and two kinds of model simulations, one of which assimilated GNSS RO into analysis fields and the other did not, and the formulation to calculate the bending angle standard deviation. The GNSS RO observation error improvement mainly occurs in the upper levels of troposphere and in the stratosphere, where is almost "null space" for the earth conventional observation. GNSS RO observations can "see" the vertical structures of the "null space".

3. GNSS RO observations impact experiments

3.1. Analysis fields biases experiment

The analysis fields biases experiment is a statistical process for the biases of geopotential height and temperature differences between unassimilated background fields and radiosonde measurements, and between the analysis fields assimilated with a new type of observation and radiosonde measurements. Its purpose is to estimate the impact that the new observations bring to the analysis fields. This experiment uses radiosonde measurements as a baseline here because radiosonde measurements have small observation errors and biases in them are nearly zero. Radiosonde measurements are very close to the true values of the atmosphere. They are good enough to be the comparison and estimation standard values.

There are three experiments in the analysis fields biases experiment. (i) Control experiment (CNTL) assimilated all the conventional observations and satellite radiance observations except GNSS RO observations. (ii) GNSS RO observations assimilation experiment (GNSSE) assimilated all the available GNSS RO observations on the basis of control experiment with full levels which are 247 levels for GRAS and 300 levels for COSMIC and others. (iii) Thinned GNSS RO observations assimilation experiment (thinned-GNSSE) assimilated all the available GNSS RO observations whose levels are thinned near the model levels to 68 levels according to control experiment. The thinning procedure is expected to reduce the vertical and horizontal correlations of the GNSS RO observations.

The experiments are performed for the period 1 August 2012–31 August 2012 using YH4DVAR data assimilation system with the observation operator of one-dimensional bending angle implemented in it.[9] Figure 5 shows the biases of geopotential height and temperature in the Northern Hemisphere. The black dashed line shows the control experiment result. The black solid line represents the GNSSE experiment result, and the red solid line gives the result of thinned-GNSSE experiment.

The bias values of geopotential height analysis fields in the Northern Hemisphere exhibit little impact at the surface or at the low troposphere, decrease from the height of 500 hPa until the top level of the model. The values' decreasing denotes the impact of GNSS RO observations is increasing. The impact reaches a maximum at the height of 60 hPa. The impact for temperature is obviously lower than that for geopotential height, but some positive impact can still be seen from Fig. 5(b).

The biases for geopotential height and temperature in the Southern Hemisphere are given in Fig. 6.

Comparing Fig. 5(a) with Fig. 6(a), the geopotential height correction that GNSS RO observations bring in the Southern Hemisphere is larger that in the Northern Hemisphere. The main reason for this phenomenon is that the number of conventional observations in the Southern Hemisphere is much smaller than the number in the Northern Hemisphere. This is also the reason for the bias in the Southern Hemisphere being larger than that in the Northern Hemisphere. As the introduction of GNSS RO observations shows, the influence that makes in the Southern Hemisphere is larger than that in the Northern Hemisphere.

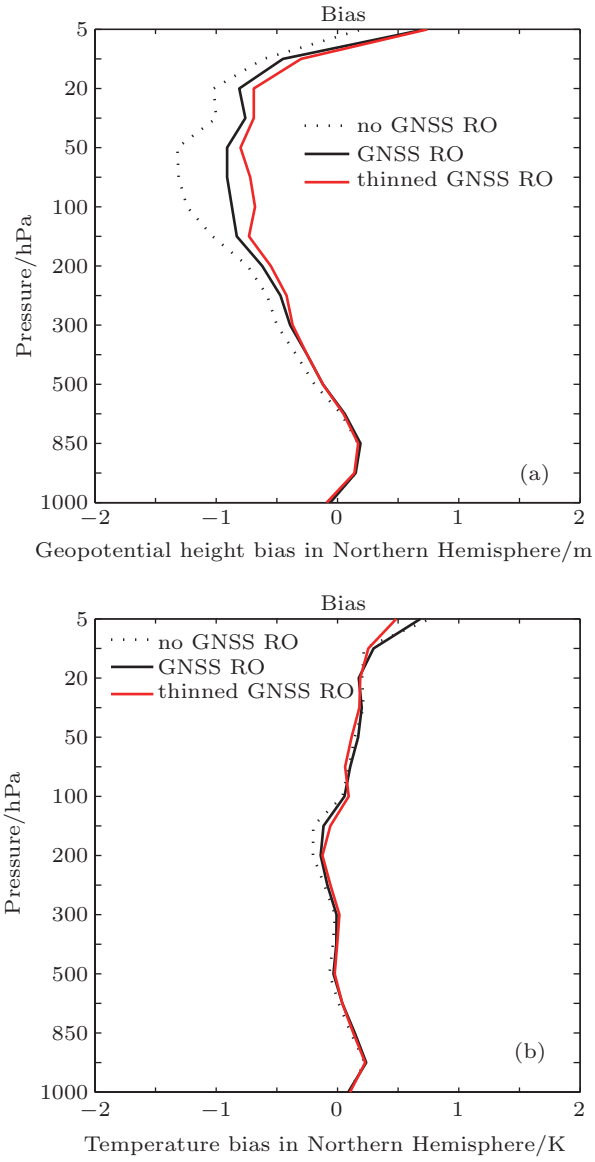

Fig. 5. (color online) Geopotential height (a) and temperature (b) analysis bias in Northern Hemisphere.

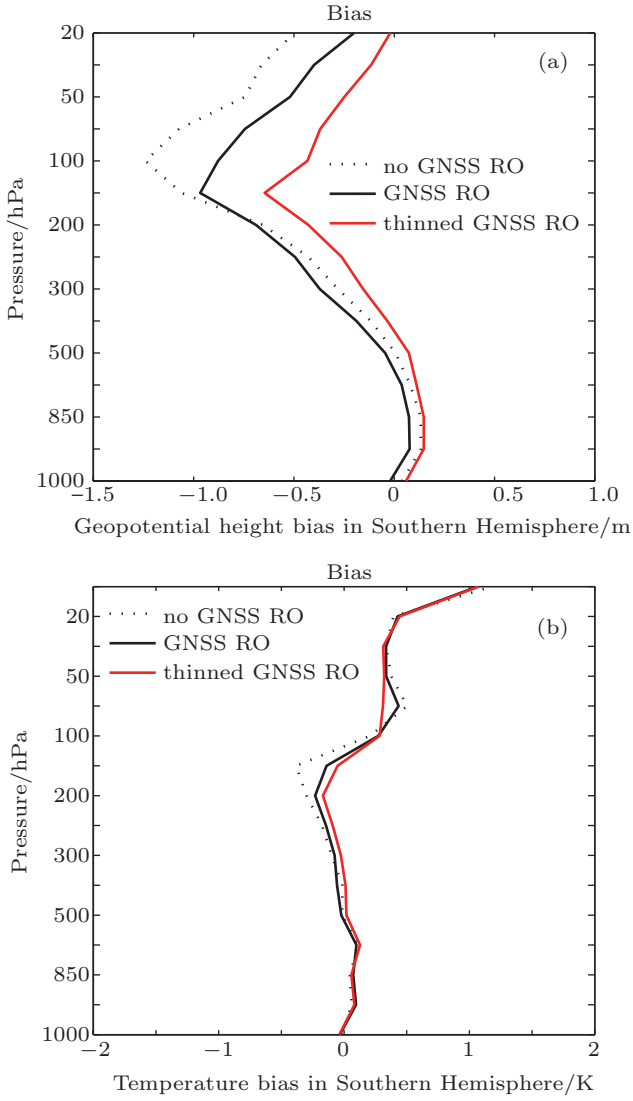

Fig. 6. (color online) Geopotential height (a) and temperature (b) analysis bias in Southern Hemisphere.

Besides, the improvement of thinned-GNSSE experiment bias values that assimilated the thinned-level GNSS RO profiles compared with GNSSE experiment values assimilated the full-level GNSS RO profiles is obviously demonstrated in Fig. 5 and Fig. 6. Every full-level GNSS RO profile has 300 (or 247) vertical levels, which are much more than the model's vertical levels. As a result, there are strong observational correlations between the vertical levels, just as the horizontal correlations in background error covariance matrix. The thinning procedure assures that the observation profile levels is close to the model levels between the height of 2 km and the top height of 50 km, considering the observations quality control strategy. Through thinning, the observation profile levels are reduced to 68 levels from 300 levels (maybe from 247 levels). With the reduction of profile levels, the correlations between vertical levels reduce to a level that could be easily seen in the experiment results in Fig. 5 and Fig. 6.

3.2. Forecast skill experiment

The assimilation of GNSS RO bending angle observations with GBAO operator gives a good improvement in NWP forecast skills. There are two experiments in this section. The control experiment (with label "no-gps") assimilated all the conventional observations and satellite radiance observations, except GNSS RO observations. The comparison experiment (with label "gps") assimilated all the additional GNSS RO observations in the light of control experiment. The experiments performed in the period 1 October–31 October 2011. Figures 7 and 8 show the WMO standard monthly average statistical tests of geopotential height (gpm) in Tropical areas for October 2011. Figures 7(a) and 8(a) show the root-mean-square (RMS) errors for Tropical and Asian areas separately at the height of 850 hPa. Figures 7(b) and 8(b) show the anomaly correlations (%) for Tropical and Asia areas separately at the height of 850 hPa. In Fig. 7 and Fig. 8, the green line with stars on it represents the control experiment results and the blue line with circles on it represents the comparison experiment results.

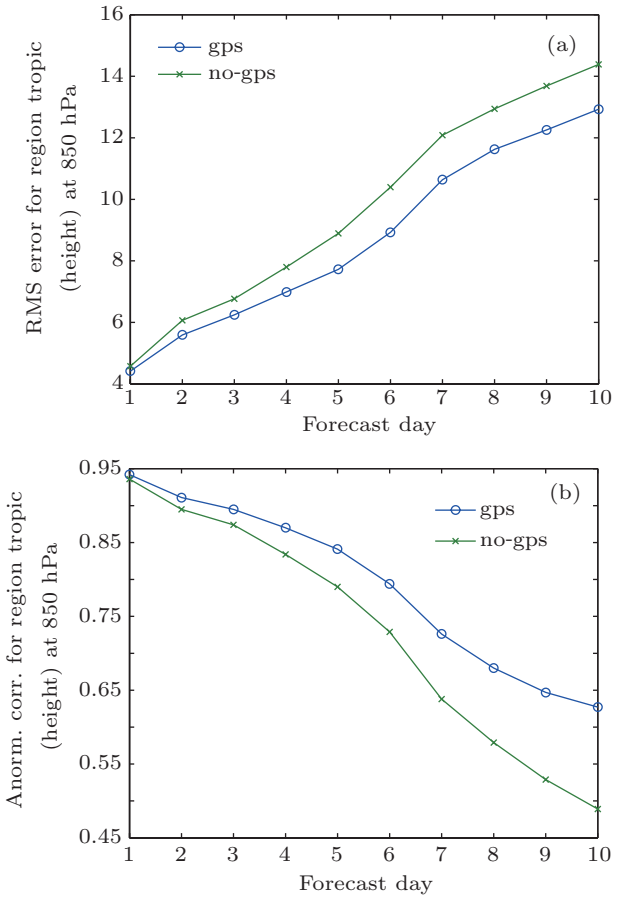

Fig. 7. (color online) Tropical geopotential height RMS (a) and anomaly correlations (b) at 850 hPa in October 2011.

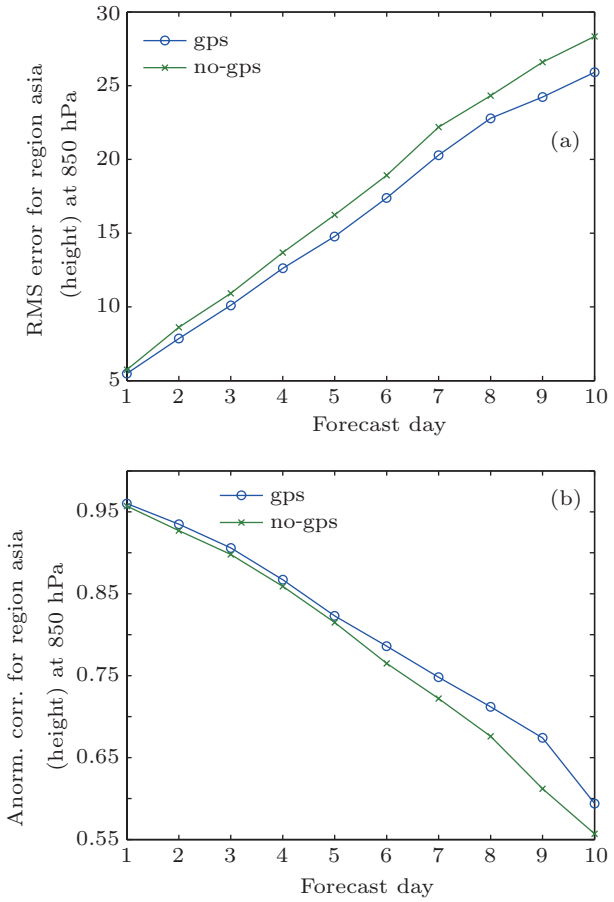

Fig. 8. (color online) Asia region geopotential height RMS (a) and anomaly correlations (b) at 850 hPa in October 2011.

Figures 7 and 8 demonstrate that GNSS RO observations have a remarkable positive impact on the forecasting skills, especially after the fifth day. The anomaly correlations for Tropical at the height of 850 hPa in October improve 17% at the eighth day. That is an exciting result which indicates the importance of GNSS RO observations to the data assimilation system. Through the comparison between Fig. 7 and Fig. 8, a phenomenon that the improvement in Tropical area is larger than that in Asia area is found. The main reason for this is that there are more conventional observations in Asia area than in Tropical area, and the impact of GNSS RO data to the data assimilation system in Asia area becomes smaller. Similar results could be found in other months, although the experiments only gave one-month results. Further, the addition of GNSS RO measurements improves the performance of microwave radiance measurements to the data assimilation system.

4. Typhoon forecast impact experiment

From Section 3, we can see that GNSS RO data have an obvious positive impact on NWP forecast skills, especially for the statistical scores of temperature and geopotential height fields. Another question arises: What is the impact of GNSS RO data on some specified weather procedures? This part the experiment was performed to verify the impact of GNSS RO measurements on analysis and prediction of the typhoon. A typhoon is one of the most harmful and damageable weather processes in China and other areas in the world. Every year, it causes great casualties and economic losses. If we can make the path and intensity forecasts of a typhoon more accurate, the social and economic benefits would be astonishing.[14]

Typhoon "BOLAVEN" was the fifteenth typhoon in 2012. It influenced South China Sea and East China Sea from 25 August 2012 to 28 August 2012. In this experiment the first guess field was offered by YH4DVAR data assimilation system, and the forecast model was used to generate the typhoon forecasts. The forecast start time is 00z 25 August 2012, and the end time is 18z 27 August 2012. The forecast time interval was three hours. The control experiment assimilated conventional observations and ATOVS satellite observations, and the comparison experiment assimilated additional GNSS RO observations according to the control experiment.

Figure 9 gives three paths of "BOLAVEN", the red solid line is the observation path, and the blue solid line with label 1 is the comparison experiment typhoon path with GNSS RO observations assimilated, the green solid line with label 2 is the

control experiment typhoon path, respectively. After assimilation of GNSS RO data effectively and correctly, the typhoon path becomes more stable and the development of typhoon is more close to the observed path.

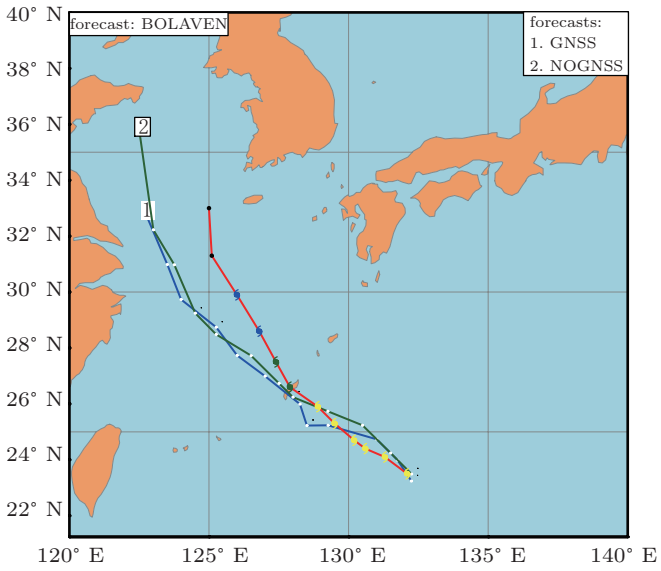

Fig. 9. (color online) The three paths of typhoon "BOLAVEN" (red: observation, green: no GNSS RO, blue: with GNSS RO).

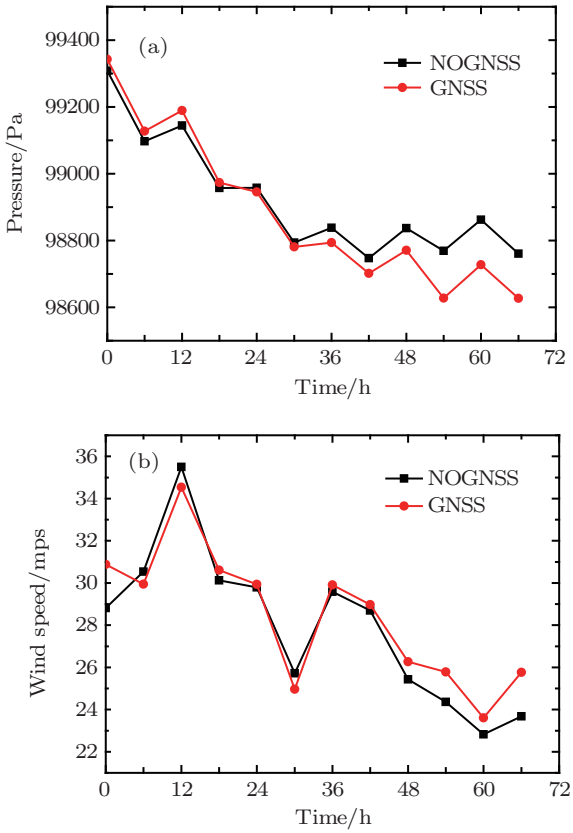

Fig. 10. (color online) The central pressure (a) and max wind speed (b) of typhoon "BOLAVEN".

Figure 10 compares the central pressure and maximum wind speed of the control experiment and comparison experiment. In Fig. 10, the red line with circle represents the comparison experiment's typhoon central pressure and maximum wind speed, and the black line with rectangle denotes the results of the control experiment. The typhoon intensity increases as the forecast time lengthens. This makes the typhoon intensity closer to the observed one. The conclusion is that the positive impact of GNSS RO observations on a typhoon can easily be achieved by the path and intensity forecasts.

5. Conclusions

The data assimilation technique for GNSS RO measurements have received much attention because of its excellent characteristics and the increasing data volume. First of all, we introduced the operational radio occultation constellations and some error and distribution characteristics of the radio occultation data in this article. The GNSS RO observations are not uniformly distributed. They vary with the latitude, especially when there are not enough observations (as expected in Tropical areas). GNSS RO data assimilations can have impact mainly on the upper troposphere and on stratosphere.

Then, we performed two experiments to evaluate the impact of GNSS RO measurements on numerical weather prediction. The analysis fields biases experiment shows that the GNSS RO has a positive influence on atmospheric fields of geopotential height and temperature in the Extratropics. It is better to use the thinned-level measurements than the full-level measurements because of the correlations between the vertical levels. The forecast skill experiment shows that the GNSS RO measurements can reduce the root-mean-square errors and increase the anomaly correlations in Tropical and Asia regions, especially after the fifth day. Then, we simulated the typhoon "BOLAVEN" through the typhoon impact experiment. The adding of GNSS RO measurements makes the strength of "BOLAVEN" larger and makes its path better. The strength and path are closer with the observed ones.

Although we can draw a conclusion for the impact of GNSS RO measurements assimilation, we do not know if there exists a threshold that could make the GNSS RO measurements reach a status of saturation. ECMWF has done some significant work using EDA method.[15,16] So, we will conduct an OSSE experiment to examine the analysis error as a function of simulated observation number in our future work. We can foresee that the number of GNSS RO measurements is increasing exponentially with the completed systems of "Galileo" of Europe, "Glonass" system of Russian, and the "Compass" system of China, which is finally being built. In addition, various radio occultation constellation missions are being carried out. The future of GNSS RO is amazing.

After all, the accuracy of one-dimensional bending angle operator is too low, and the "tangent point" drift is not considered in the corresponding calculation.[17,18] Future work will

focus on the improvement of the accuracy of observation operator. A two-dimensional bending angle operator is being considered to be added into YH4DVAR system. The "tangent point" drift will be cancelled by some of these changes.[19–21]

References

[1] Kursinski E, Hajj G, Bertiger W, Leroy S, Meehan T, Romans L, Schofield J, McCleese D, Melbourne W, Thornton C, Yunck T, Eyre J and Nagatani R 1996 *Science* **271** 1107

[2] Syndergaard S, Kursinski E, Herman B, Lane E and Flittner 2004 *Mon. Wea. Rev.* **133** 2650

[3] Healy S, Eyre J, Hamrud M and Thépaut J 2007 *Quart. J. Roy. Meteorol. Soc.* **133** 1213

[4] Healy S and Thépaut J 2006 *Quart. J. Roy. Meteorol. Soc.* **132** 605

[5] Anthes R, Bernhardt P, Chen Y, Cucurull L, Dymond K, Ector D, Healy S, Ho S, Hunt Y, Kuo D, Liu H, Manning C, McCormick, Meehan T, Randel W, Rocken C, Schreiner W, Sokolovskiy S, Syndergaard S, Thompson D, Trenberth K, Wee T, Yen N and Zeng Z 2008 *Bull. Am. Meteor. Soc.* **89** 313

[6] Zhang W M, Cao X Q and Song J Q 2012 *Acta Phys. Sin* **61** 249202 (in Chinese)

[7] Cao X Q, Zhang W M and Song J Q 2012 *Acta Phys. Sin* **61** 020507 (in Chinese)

[8] Zhang W M 2006 *Research on Data Assimilation and Its Parallel Implementation* (Ph. D. Thesis) (Changsha: National University of Defense Technology) (in Chinese)

[9] Zhu M B, Zhang W M and Cao X Q 2013 *Acta Phys. Sin* **62** 189203 (in Chinese)

[10] Cucurull L, Derber J and Purser R 2012 *J. Geophys. Res.* (in press)

[11] Cardinali C, Daescu D, Healy S, Dahoui M, Radnoti G and Fouilloux A 2011 *ECMWF Seminar* (in report)

[12] Marbouty D and Healy S 2011 *ICGPSRO* (in report)

[13] Rüeger J 2002 *Refractive Index Formulae for Electronic Distance Measurement with Radio and Millimetre Waves* (Unisurv Rep. S-68) (Sydney: University of New South Wales)

[14] Yang W X, Chu Y L and Ran L K 2010 *Chin. Phys. B* **19** 079201

[15] Harnisch F, Healy S, Bauer P and English S 2013 *ECMWF Technical Memorandum* **693** (submitted to *Monthly Weather Review*)

[16] Bauer P, Radnóti G, Healy S and Cardinali C 2013 *ECMWF Technical Memorandum* **692** (submitted to *Monthly Weather Review*)

[17] Huang S X, Zhao X F and Sheng Z 2009 *Chin. Phys. B* **18** 5084

[18] Zhao X F, Huang S X and Sheng Z 2010 *Chin. Phys. B* **19** 049201

[19] Zhao X F and Huang S X 2011 *Chin. Phys. B* **20** 029201

[20] Zhang J P, Wu Z S, Zhao Z W, Zhang Y S and Wang B 2012 *Chin. Phys. B* **21** 109202

[21] Foelsche U, Syndergaard S, Fritzer J and Kirchengast 2011 *Atmos. Meas. Tech.* **4** 189